

Link prediction in dynamic networks using random dot product graphs

Francesco Sanna Passino¹, Anna S. Bertiger², Joshua C. Neil², and Nicholas A. Heard¹

¹Department of Mathematics, Imperial College London

²Microsoft Defender Advanced Threat Protection, Microsoft Corporation, Redmond (WA)

July 4, 2022

Abstract

The problem of predicting links in large networks is a crucial task in a variety of practical applications, including social sciences, biology and computer security. In this paper, statistical techniques for link prediction based on the popular random dot product graph model are carefully presented, analysed and extended to dynamic settings. Motivated by a practical application in cyber-security, this paper demonstrates that random dot product graphs not only represent a powerful tool for inferring differences between multiple networks, but are also efficient for prediction purposes and for understanding the temporal evolution of the network. The probabilities of links are obtained by fusing information at multiple levels of resolution: time series models are used to score connections at the edge level, and spectral methods provide estimates of latent positions for each node. In this way, traditional link prediction methods, usually based on decompositions of the entire network adjacency matrix, are extended using edge-specific information. The methods presented in this article are applied to a number of simulated and real-world computer network graphs, showing promising results.

Keywords – adjacency spectral embedding, dynamic networks, link prediction, random dot product graph.

1 Introduction

Link prediction is defined as the task of predicting the presence of an edge between two nodes in a network, based on latent characteristics of edges and nodes (Liben-Nowell and Kleinberg, 2007). The problem of link prediction has been widely studied in the literature (for some examples, see Lü and Zhou, 2011; Menon and Elkan, 2011) and has relevant applications in a variety of different fields. In this paper, the discussion about link prediction methods is motivated by ap-

plications in cyber-security and computer network monitoring (Neil et al., 2013; Heard et al., 2018; Jeske et al., 2018). The ability to correctly predict and associate anomaly scores with the connections in a network is crucial for the cyber-defence of enterprises. In cyber settings, adversaries may introduce changes in the structure of a dynamic graph (an enterprise network) in the course of their attack. Therefore, predicting links in order to identify significant deviations in expected behaviour could lead to the detection of an otherwise extremely damaging breach to an enterprise. In particular, it is necessary to correctly score *new links* (Metelli and Heard, 2019), representing previously unobserved connections. The task is particularly important since it is common to observe malicious activity associated with new links, and it is therefore crucial to understand the normal process of link formation in order to detect a cyber-attack. Furthermore, computer network graphs tend to be extremely large, and computationally efficient methods are hence required.

In this article, it is assumed that snapshots of a dynamic network are observed at discrete time points $t = 1, \dots, T$, obtaining a sequence of graphs $\mathbb{G}_t = (V, E_t)$. The set V represents the set of nodes, which is invariant over time. On the other hand, the set E_t is a time dependent edge set, where $(i, j) \in E_t$, $i, j \in V$, if i connected to j at least once during the time period $(t - 1, t]$. Each snapshot of the graph can be characterised by the adjacency matrix $\mathbf{A}_t \in \{0, 1\}^{n \times n}$, where $n = |V|$ and for $1 \leq i, j \leq n$, $A_{ijt} = \mathbf{1}_{E_t}\{(i, j)\}$, such that $A_{ijt} = 1$ if a link between the nodes i and j exists in $(t - 1, t]$, and $A_{ijt} = 0$ otherwise. The graph is said to be undirected if $(i, j) \in E_t \iff (j, i) \in E_t$ and \mathbf{A}_t is constrained to be symmetric; otherwise, the graph is said to be directed. Furthermore, it will be assumed that the graph has no self-edges, implying \mathbf{A}_t is a hollow matrix. Similarly, bipartite graphs $\mathbb{G}_t = (V_1, V_2, E_t)$ can be represented using two node sets V_1 and V_2 , and rectangular adjacency matrices $\mathbf{A}_t \in \{0, 1\}^{n_1 \times n_2}$, $n_1 = |V_1|$, $n_2 = |V_2|$, where $A_{ijt} = 1$ if $i \in V_1$ connects to $j \in V_2$ in $(t - 1, t]$.

The main objective of this work is to discuss reliable statistical methods for prediction of \mathbf{A}_{t+1} for any $t \in \{1, \dots, T\}$, given the history of the process $\mathbf{A}_1, \dots, \mathbf{A}_t$. Following the nomenclature of Dunlavy et al. (2011), the problem is described as *temporal link prediction*. This problem fundamentally differs from the standard *missing link prediction* problem, widely analysed in the literature (see, for example, Clauset et al., 2008), which aims at filling in missing entries in a single incomplete graph adjacency matrix.

Traditionally, the temporal link prediction task is tackled using tensor decompositions (Dunlavy et al., 2011). Dynamic models have also been proposed in the literature of Poisson matrix factorisation and recommender systems (Charlin et al., 2015; Hosseini et al., 2018), and extended to Bayesian tensor decompositions (Schein et al., 2015, 2016). In general, including time has been shown to significantly improve the predictive performance in a variety of model settings, for example stochastic blockmodels (Ishiguro et al., 2010; Xu and Hero III, 2014) and mixed membership stochastic blockmodels (Xing et al., 2010). More generic latent space models for dynamic networks have also been extensively discussed in the literature (Sarkar and Moore, 2006; Durante and Dunson, 2014; Krivitsky and Handcock, 2014; Sewell and Chen, 2015), and are usually based on Markovian assumptions.

In this article, temporal link prediction techniques based on *random dot product graphs* (RDPG, Young and Scheinerman, 2007) are discussed and compared. RDPGs are a tractable class of *latent position models* (Hoff et al., 2002), and have been extensively studied because of their analytical tractability (Athreya et al., 2018). Each node i is given a latent position \mathbf{x}_i in a d -dimensional latent space \mathbb{X} such that $\mathbf{x}^\top \mathbf{x}' \in [0, 1] \forall \mathbf{x}, \mathbf{x}' \in \mathbb{X}$. The edges between pairs of nodes are generated independently, with probability of a link between nodes i and j obtained through the inner product $\langle \cdot, \cdot \rangle$ on $\mathbb{X} \times \mathbb{X}$, written $\mathbb{P}(A_{ij} = 1) = \mathbf{x}_i^\top \mathbf{x}_j$. In matrix notation, the latent position can be grouped in a $n \times d$ matrix $\mathbf{X} = [\mathbf{x}_1, \dots, \mathbf{x}_n]^\top \in \mathbb{X}^n$, and the expected value of a single adjacency matrix \mathbf{A} can be expressed as $\mathbb{E}(\mathbf{A}) = \mathbf{X}\mathbf{X}^\top$.

RDPGs have not been formally extended to a dynamic setting, but models for multiple heterogeneous graphs on the same node set have recently been proposed in the literature. Early examples discuss methods for clustering and community detection with multiple graphs (Tang et al., 2009; Shiga and Mamitsuka, 2012; Dong et al., 2014). More recently, the focus has been on testing for differences in brain connectivity networks (Arroyo-Reli3n et al., 2017; Ginestet et al., 2017; Levin et al., 2017; Kim and Levina, 2019). Levin et al. (2017) propose an *omnibus* embedding in which the different graphs are jointly embedded into a common latent space, providing distinct representations for each graph and for each node. Wang et al. (2019) propose the *multiple random eigen graph* (MREG) model, where a common set of d -dimensional latent features \mathbf{X} is shared between the graphs, and the inner product between the latent positions is weighted differently

across the networks, obtaining $\mathbb{E}(\mathbf{A}_t) = \mathbf{X}\mathbf{R}_t\mathbf{X}^\top$, where \mathbf{R}_t is a $d \times d$ diagonal matrix. Nielsen and Witten (2018) propose the *multiple random dot product graph* (multi-RDPG), which more naturally extends the RDPG to the multi-graph setting. Their formulation is similar to the MREG of Wang et al. (2019), but \mathbf{X} is modelled as an orthogonal matrix, and \mathbf{R}_t is constrained to be positive semi-definite. The model is further extended in *common subspace independent edge* (COSIE) graphs (Arroyo-Reli3n et al., 2019), in which \mathbf{R}_t does not need to be a diagonal matrix. Durante et al. (2017); Durante and Dunson (2018) propose a Bayesian nonparametric framework, interpreting the network snapshots as realisations from a common network-valued random variable, modelled through an unknown probability mass function, characterised using a mixture of low-rank factorisations. Unfortunately, the Bayesian nonparametric scheme cannot be scaled to large networks.

In this work, some of the methods for multiple graph inference in random dot product graphs will be compared for temporal link prediction, combining the information obtained at the node level via spectral methods with edge specific characteristics inferred from the observed graphs. It will be shown that this approach significantly improves the predictive performance of RDPG models, especially when the network presents a seasonal or temporal evolution. This is among the first papers to tackle the combination of node and edge characteristics obtained from RDPG embeddings in large time-evolving networks.

The article is organised as follows: Section 2 introduces the main statistical tools used in this paper: the generalised random dot product graph (GRDPG) and adjacency spectral embeddings. Methods for link prediction based on random dot product graphs are discussed in Section 3, followed by a discussion on alignment of individual embeddings using generalised Procrustes analysis in Section 4. Section 5 presents techniques to improve the predictive performance of the RDPG models, based on edge-specific information. Results and applications are finally discussed in Section 6.

2 Random dot product graphs and adjacency spectral embedding

In this section, the generalised random dot product graph and methods for estimation of the latent positions are formally introduced. Suppose $\mathbf{A} \in \{0, 1\}^{n \times n}$ is a symmetric adjacency matrix of an undirected graph with n nodes.

Definition 1 (Generalised random dot product graph (Rubin-Delanchy et al., 2017), GRDPG). *Let d_+ and d_- be non-negative integers such that $d = d_+ + d_-$. Let $\mathbb{X} \subseteq \mathbb{R}^d$ such that $\forall \mathbf{x}, \mathbf{x}' \in \mathbb{X}, 0 \leq \mathbf{x}^\top \mathbf{I}(d_+, d_-) \mathbf{x}' \leq 1$, where*

$$\mathbf{I}(p, q) = \text{diag}(\underbrace{1, \dots, 1}_p, \underbrace{-1, \dots, -1}_q).$$

Let \mathcal{F} be a probability measure on \mathbb{X} , $\mathbf{A} \in \{0, 1\}^{n \times n}$ be a symmetric matrix and $\mathbf{X} = (\mathbf{x}_1, \dots, \mathbf{x}_n)^\top \in \mathbb{X}^n$. Then $(\mathbf{A}, \mathbf{X}) \sim \text{GRDPG}_{d_+, d_-}(\mathcal{F})$ if $\mathbf{x}_1, \dots, \mathbf{x}_n \stackrel{iid}{\sim} \mathcal{F}$ and for $i < j$, independently

$$\mathbb{P}(A_{ij} = 1) = \mathbf{x}_i^\top \mathbf{I}(d_+, d_-) \mathbf{x}_j.$$

Adjacency spectral embedding (ASE) provides consistent estimates of the latent positions in a GRDPG (Rubin-Delanchy et al., 2017).

Definition 2 (Adjacency spectral embedding – ASE). For $d \in \{1, \dots, n\}$, consider the spectral decomposition

$$\mathbf{A} = \hat{\Gamma} \hat{\Lambda} \hat{\Gamma}^\top + \hat{\Gamma}_\perp \hat{\Lambda}_\perp \hat{\Gamma}_\perp^\top,$$

where $\hat{\Lambda}$ is a $d \times d$ diagonal matrix containing the top d eigenvalues in magnitude, in decreasing order, $\hat{\Gamma}$ is a $n \times d$ matrix containing the corresponding orthonormal eigenvectors, and the matrices $\hat{\Lambda}_\perp$ and $\hat{\Gamma}_\perp$ contain the remaining $n - d$ eigenvalues and eigenvectors. The adjacency spectral embedding $\hat{\mathbf{X}} = [\hat{\mathbf{x}}_1, \dots, \hat{\mathbf{x}}_n]^\top$ of \mathbf{A} in \mathbb{R}^d is

$$\hat{\mathbf{X}} = \hat{\Gamma} |\hat{\Lambda}|^{1/2} \in \mathbb{R}^{n \times d},$$

where the operator $|\cdot|$ applied to a matrix returns the absolute value of its entries.

A common alternative to ASE is the Laplacian spectral embedding (LSE), which considers the eigendecomposition of the Laplacian matrix $\mathbf{L} = \mathbf{D}^{-1/2} \mathbf{A} \mathbf{D}^{-1/2}$, where $\mathbf{D} = \text{diag}(\sum_{i=1}^n A_{ij})$ is the degree matrix.

If the graph is directed, and the adjacency matrix is not symmetric, it could be implicitly assumed that the generating model is $\mathbb{P}(A_{ij} = 1) = \mathbf{x}_i^\top \mathbf{y}_j$, $\mathbf{x}_i, \mathbf{y}_j \in \mathbb{X}$. In this case, the embeddings can be estimated using the singular value decomposition (SVD).

Definition 3 (Adjacency embedding of the directed graph – DASE). Given a directed graph with adjacency matrix $\mathbf{A} \in \{0, 1\}^{n \times n}$, and a positive integer d , $1 \leq d \leq n$, consider the singular value decomposition

$$\mathbf{A} = \begin{bmatrix} \hat{\mathbf{U}} & \hat{\mathbf{U}}_\perp \end{bmatrix} \begin{bmatrix} \hat{\mathbf{D}} & \mathbf{0} \\ \mathbf{0} & \hat{\mathbf{D}}_\perp \end{bmatrix} \begin{bmatrix} \hat{\mathbf{V}}^\top \\ \hat{\mathbf{V}}_\perp^\top \end{bmatrix} = \hat{\mathbf{U}} \hat{\mathbf{D}} \hat{\mathbf{V}}^\top + \hat{\mathbf{U}}_\perp \hat{\mathbf{D}}_\perp \hat{\mathbf{V}}_\perp^\top,$$

where $\hat{\mathbf{D}} \in \mathbb{R}_+^{d \times d}$ is diagonal matrix containing the top d singular values in decreasing order, $\hat{\mathbf{U}} \in \mathbb{R}^{n \times d}$ and $\hat{\mathbf{V}} \in \mathbb{R}^{n \times d}$ contain the corresponding left and right singular vectors, and the matrices $\hat{\mathbf{D}}_\perp$, $\hat{\mathbf{U}}_\perp$, and $\hat{\mathbf{V}}_\perp$ contain the remaining $n - d$ singular values and vectors. The d -dimensional directed adjacency embedding of \mathbf{A} in \mathbb{R}^d , is defined as the pair

$$\hat{\mathbf{X}} = \hat{\mathbf{U}} \hat{\mathbf{D}}^{1/2}, \quad \hat{\mathbf{Y}} = \hat{\mathbf{V}} \hat{\mathbf{D}}^{1/2}.$$

Hence, each node has two different latent positions, representing the behaviour of the node as source or destination of the link. Note that DASE in Definition 3 can be also extended to bipartite graphs (Dhillon, 2001).

3 Dynamic link prediction in random dot product graphs

Given a time series of network adjacency matrices $\mathbf{A}_1, \mathbf{A}_2, \dots, \mathbf{A}_T$, the objective is to correctly predict \mathbf{A}_{T+1} . Sharan and Neville (2008); Scheinerman and Tucker (2010); Dunlavy et al. (2011) suggest to analyse a collapsed version $\tilde{\mathbf{A}}$ of the adjacency matrices:

$$\tilde{\mathbf{A}} = \sum_{t=1}^T \psi_{T-t+1} \mathbf{A}_t, \quad (3.1)$$

where ψ_1, \dots, ψ_T is a sequence of weights. Scheinerman and Tucker (2010) propose to consider an average adjacency matrix, setting $\psi_t = 1/T \forall t = 1, \dots, T$, which provides the maximum likelihood estimate of $\mathbb{E}(\mathbf{A}_t)$ if $\mathbf{A}_1, \dots, \mathbf{A}_T$ are sampled independently from the same distribution Bernoulli($\mathbf{X}\mathbf{X}^\top$). Tang et al. (2019) compares the performance of (3.1) and a low-rank approximation based on spectral embedding for estimation of $\mathbb{E}(\mathbf{A}_t)$. The main limitation of such a model is that it is assumed that the graphs are sampled independently from the same distribution, without any temporal evolution of the network. Furthermore, if (3.1) is used, it is assumed that all the possible edges of the adjacency matrix follow the same dynamics, controlled by the parameters ψ_1, \dots, ψ_T . Taking the ASE $\hat{\mathbf{X}} = [\hat{\mathbf{x}}_1, \dots, \hat{\mathbf{x}}_n]$ of $\tilde{\mathbf{A}}$ gives a method to estimate the scores:

$$\mathbf{S} = \hat{\mathbf{X}} \hat{\mathbf{X}}^\top. \quad (3.2)$$

Note that, for simplicity, the inner product is not weighted by the matrix $\mathbf{I}(d_+, d_-)$, hence it is implicitly assumed in (3.2) that $d = d_+$ and $d_- = 0$. The notation can be naturally extended to the case $d_- \neq 0$.

Alternatively, it is possible to consider the individual ASEs $\hat{\mathbf{X}}_1, \hat{\mathbf{X}}_2, \dots, \hat{\mathbf{X}}_T$ of $\mathbf{A}_1, \mathbf{A}_2, \dots, \mathbf{A}_T$. The inner product is invariant to orthogonal rotations of the embeddings, so it is still possible to calculate an averaged score:

$$\mathbf{S} = \frac{1}{T} \sum_{t=1}^T \hat{\mathbf{X}}_t \hat{\mathbf{X}}_t^\top. \quad (3.3)$$

An alternative option is to obtain an averaged embedding $\bar{\mathbf{X}}$ based on $\hat{\mathbf{X}}_1, \hat{\mathbf{X}}_2, \dots, \hat{\mathbf{X}}_T$, and use it for calculating the scores. This procedure is particularly complex, since the embeddings are not directly comparable. In the GRDPG setting, $\mathbb{E}(\mathbf{A}) = \mathbf{X} \mathbf{I}(d_+, d_-) \mathbf{X}^\top = (\mathbf{X} \mathbf{Q}) \mathbf{I}(d_+, d_-) (\mathbf{X} \mathbf{Q})^\top \forall \mathbf{Q} \in \mathcal{O}(d_+, d_-)$, where $\mathcal{O}(d_+, d_-)$ is the indefinite orthogonal group with signature (d_+, d_-) , and therefore it is first necessary to align the individual embeddings before performing any statistical comparison between them. Furthermore, it is required to use the same values of d_+ and d_- for each embedding for the procedure to be meaningful, which implies that the ASE in Definition 2 must be accordingly modified

to look at the top d_+ and d_- eigenvalues at both ends of the spectrum. A technique to jointly align $\hat{\mathbf{X}}_1, \hat{\mathbf{X}}_2, \dots, \hat{\mathbf{X}}_T$, provided that the same values of d_+ and d_- are used, is discussed in Section 4. If an averaged embedding $\bar{\mathbf{X}}$ is obtained, then the matrix of scores for prediction of \mathbf{A}_{T+1} is:

$$\mathbf{S} = \bar{\mathbf{X}}\bar{\mathbf{X}}^\top. \quad (3.4)$$

A similar scoring mechanism can be derived from the omnibus embedding (Levin et al., 2017) obtained from $\mathbf{A}_1, \mathbf{A}_2, \dots, \mathbf{A}_T$. Consider the omnibus matrix (Levin et al., 2017):

$$\tilde{\mathbf{A}} = \begin{bmatrix} \mathbf{A}_1 & \frac{\mathbf{A}_1 + \mathbf{A}_2}{2} & \dots & \frac{\mathbf{A}_1 + \mathbf{A}_T}{2} \\ \frac{\mathbf{A}_2 + \mathbf{A}_1}{2} & \mathbf{A}_2 & \dots & \frac{\mathbf{A}_2 + \mathbf{A}_T}{2} \\ \vdots & \vdots & \ddots & \vdots \\ \frac{\mathbf{A}_T + \mathbf{A}_1}{2} & \frac{\mathbf{A}_T + \mathbf{A}_2}{2} & \dots & \mathbf{A}_T \end{bmatrix}. \quad (3.5)$$

The ASE $\hat{\mathbf{X}}$ of $\tilde{\mathbf{A}}$ gives T latent positions for each node. The individual estimates $\hat{\mathbf{X}}_t = [\hat{x}_{1t}, \dots, \hat{x}_{nt}]$ of the latent positions for the t -th adjacency matrix are represented by the submatrix formed by the estimates between the $(t-1)n$ -th and tn -th row of $\hat{\mathbf{X}}$. Then, from the time series $\hat{\mathbf{X}}_1, \hat{\mathbf{X}}_2, \dots, \hat{\mathbf{X}}_T$ of omnibus embeddings, a matrix of scores can be obtained using either (3.3) or (3.4). Note that in this case the individual embeddings are directly comparable and it is not required to perform an alignment step. On the other hand, note that the scoring mechanism based on the omnibus embedding cannot easily be updated when new graphs $\mathbf{A}_{T+1}, \mathbf{A}_{T+2}, \dots$ are available, since the matrix $\tilde{\mathbf{A}}$ and the embedding must be recomputed, generating a different sequence of node embeddings which is not necessarily equal to the time series of embeddings calculated when only T matrices were available. Finally, the idea of omnibus embedding can be also easily extended to directed and bipartite graphs, constructing the matrix $\tilde{\mathbf{A}}$ in an analogous way and then calculating the DASE.

In conclusion, the more parsimonious COSIE model (Arroyo-Reli3n et al., 2019) is considered. In COSIE networks, the latent positions are assumed to be common across the T snapshots of the graph, but the link probabilities are scaled by a time-varying matrix $\mathbf{R}_t \in \mathbb{R}^{d \times d}$. This gives:

$$\mathbb{E}(\mathbf{A}_t) = \mathbf{X}\mathbf{R}_t\mathbf{X}^\top.$$

The common latent positions \mathbf{X} and the time series of weighting matrices $\mathbf{R}_1, \dots, \mathbf{R}_T$ can be estimated via multiple adjacency spectral embedding (MASE, Levin et al., 2017), defined below.

Definition 4 (Multiple adjacency spectral embedding – MASE (Levin et al., 2017)). *Given a sequence of network adjacency matrices $\mathbf{A}_1, \dots, \mathbf{A}_T$, and an integer $d \in \{1, \dots, n\}$,*

obtain the individual ASEs $\hat{\mathbf{X}}_t = \hat{\Gamma}_t|\hat{\Lambda}_t|^{1/2} \in \mathbb{R}^{n \times d}$. Then, construct the $n \times Td$ matrix

$$\tilde{\Gamma} = [\hat{\Gamma}_1, \dots, \hat{\Gamma}_T] \in \mathbb{R}^{n \times Td},$$

and consider its singular value decomposition

$$\tilde{\Gamma} = \hat{\mathbf{U}}\hat{\mathbf{D}}\hat{\mathbf{V}}^\top + \hat{\mathbf{U}}_\perp\hat{\mathbf{D}}_\perp\hat{\mathbf{V}}_\perp^\top$$

where $\hat{\mathbf{D}} \in \mathbb{R}_+^{d \times d}$ is a diagonal matrix containing the top d singular values in decreasing order, $\hat{\mathbf{U}} \in \mathbb{R}^{n \times d}$ and $\hat{\mathbf{V}} \in \mathbb{R}^{n \times d}$ contain the corresponding left and right singular vectors, and the matrices $\hat{\mathbf{D}}_\perp, \hat{\mathbf{U}}_\perp$, and $\hat{\mathbf{V}}_\perp$ contain the remaining singular values and vectors. The d -dimensional multiple adjacency embedding of $\mathbf{A}_1, \dots, \mathbf{A}_T$ in \mathbb{R}^d is given by $\hat{\mathbf{X}} = \hat{\mathbf{U}}$, which provides an estimate of \mathbf{X} , and the sequence $\hat{\mathbf{R}}_1, \dots, \hat{\mathbf{R}}_T$, where

$$\hat{\mathbf{R}}_t = \hat{\mathbf{U}}^\top \mathbf{A}_t \hat{\mathbf{U}}.$$

For prediction, an averaged $\bar{\mathbf{R}}$ can be obtained from the time series of estimates $\hat{\mathbf{R}}_1, \dots, \hat{\mathbf{R}}_T$. Combining the estimate of the future weighting matrix with the estimate of the latent positions $\hat{\mathbf{X}}$ yields the following matrix of scores:

$$\mathbf{S} = \hat{\mathbf{X}}\bar{\mathbf{R}}\hat{\mathbf{X}}^\top. \quad (3.6)$$

Alternatively, the matrix of scores could be equivalently obtained from the time series of estimated link probabilities $\hat{\mathbf{X}}\hat{\mathbf{R}}_1\hat{\mathbf{X}}^\top, \dots, \hat{\mathbf{X}}\hat{\mathbf{R}}_T\hat{\mathbf{X}}^\top$:

$$\mathbf{S} = \frac{1}{T} \sum_{t=1}^T \hat{\mathbf{X}}\hat{\mathbf{R}}_t\hat{\mathbf{X}}^\top. \quad (3.7)$$

Note that the COSIE model has only been studied in the context of undirected graphs, but the same concept can be extended to directed and bipartite graphs, assuming $\mathbb{E}(\mathbf{A}_t) = \mathbf{X}\mathbf{R}_t\mathbf{Y}^\top$, which leads to estimates $\hat{\mathbf{R}}_t = \hat{\mathbf{U}}^\top \mathbf{A}_t \hat{\mathbf{V}}$, where $\hat{\mathbf{V}}$ is an estimate of \mathbf{Y} obtained from MASE on $\hat{\mathbf{Y}}_1, \dots, \hat{\mathbf{Y}}_T$.

In summary, multiple link prediction schemes based on random dot product graph models have been proposed and will be compared:

- collapsed weighted adjacency matrix scores – (3.2),
- scores based on individual embeddings – (3.3) and (3.4),
- omnibus scores – (3.3) and (3.4), based on the matrix representation in (3.5),
- COSIE scores – (3.6) and (3.7).

4 Generalised Procrustes alignment of individual embeddings

For prediction of the future latent positions based on individual embeddings $\hat{\mathbf{X}}_1, \dots, \hat{\mathbf{X}}_T$, it is first necessary to align the embeddings, as discussed in the previous section. A popular

method to align two matrices is Procrustes analysis (see, for example, [Dryden and Mardia, 2016](#)).

Assume that $d_- = 0$ in the GRDPG setting, implying $d = d_+$. Given two shapes $\hat{\mathbf{X}}_1, \hat{\mathbf{X}}_2 \in \mathbb{R}^{n \times d}$, Procrustes analysis aims to find the optimal rotation $P_{\hat{\mathbf{X}}_1}(\hat{\mathbf{X}}_2)$ of $\hat{\mathbf{X}}_2$ on $\hat{\mathbf{X}}_1$. The following criterion is minimised:

$$\min_{\Omega \in \mathbb{O}(d)} \left\| \hat{\mathbf{X}}_1 - \hat{\mathbf{X}}_2 \Omega \right\|_F, \quad (4.1)$$

where $\Omega \in \mathbb{O}(d)$ is an orthogonal matrix - $\Omega^\top \Omega = \Omega \Omega^\top = \mathbf{I}(d, 0)$ -, and $\|\cdot\|_F$ denotes the Frobenius norm $\|\mathbf{M}\|_F^2 = \text{tr}(\mathbf{M}^\top \mathbf{M})$, where $\text{tr}(\cdot)$ is the trace. The solution of the minimisation problem has been derived in [Schönemann \(1966\)](#), and is based on the SVD decomposition of $\hat{\mathbf{X}}_2^\top \hat{\mathbf{X}}_1$: $\hat{\mathbf{X}}_2^\top \hat{\mathbf{X}}_1 = \tilde{\mathbf{U}} \tilde{\mathbf{D}} \tilde{\mathbf{V}}^\top$. The solution is: $\Omega^* = \tilde{\mathbf{U}} \tilde{\mathbf{V}}^\top$, and it follows that the optimal rotation of $\hat{\mathbf{X}}_2$ onto $\hat{\mathbf{X}}_1$ is:

$$P_{\hat{\mathbf{X}}_1}(\hat{\mathbf{X}}_2) = \hat{\mathbf{X}}_2 \tilde{\mathbf{U}} \tilde{\mathbf{V}}^\top. \quad (4.2)$$

It is possible to use the same method to superimpose a set of T shapes $\hat{\mathbf{X}}_t \in \mathbb{R}^{n \times r}$, $t = 1, \dots, T$, choosing a reference shape $\tilde{\mathbf{X}}$, but improved results are usually obtained by *generalised Procrustes analysis* (GPA, [Gower, 1975](#)). The GPA algorithm aims at minimising the following criterion:

$$\begin{aligned} \min_{\Omega_j \in \mathbb{O}(d)} \sum_{j=1}^T \left\| \hat{\mathbf{X}}_j \Omega_j - \tilde{\mathbf{X}} \right\|_F^2 \\ \text{s.t. } \sum_{j=1}^T S^2(\hat{\mathbf{X}}_j) = \sum_{j=1}^T S^2(\hat{\mathbf{X}}_j \Omega_j), \end{aligned} \quad (4.3)$$

where, similarly to (4.1), $\Omega_j \in \mathbb{O}(d)$ is a shape-specific orthogonal matrix. Additionally, $\tilde{\mathbf{X}} \in \mathbb{R}^{n \times r}$ is a reference shape, shared across the T shapes, and $S(\cdot)$ is the *centroid size* $S(\mathbf{M}) = \|(\mathbf{I}_n - \frac{1}{n} \mathbf{1}_n \mathbf{1}_n^\top) \mathbf{M}\|_F$. The GPA algorithm solves (4.3) by iterating standard Procrustes analysis ([Dryden and Mardia, 2016](#)), after a suitable initialisation of the reference shape:

1. *update* the shapes $\hat{\mathbf{X}}_t$, performing a standard Procrustes superimposition of each $\hat{\mathbf{X}}_j$ on $\tilde{\mathbf{X}}$:

$$\hat{\mathbf{X}}_j \leftarrow \hat{\mathbf{X}}_j \tilde{\mathbf{U}}_j \tilde{\mathbf{V}}_j^\top,$$

where $\hat{\mathbf{X}}_j^\top \tilde{\mathbf{X}} = \tilde{\mathbf{U}}_j \tilde{\mathbf{D}}_j \tilde{\mathbf{V}}_j^\top$,

2. *update* the reference shape: $\tilde{\mathbf{X}} = \sum_{t=1}^T \hat{\mathbf{X}}_t$,
3. *repeat* steps 1 and 2 until the difference between two consecutive values of (4.3) is within a tolerance η .

When $d_- \neq 0$, the problem is known as *indefinite Procrustes problem*, and does not have closed form solution ([Kintzel, 2005](#)). In this setting, the criterion

$$\min_{\Omega \in \mathbb{O}(d_+, d_-)} \left\| \hat{\mathbf{X}}_1 - \hat{\mathbf{X}}_2 \Omega \right\|_F,$$

must be optimised numerically. Details about the procedure are given in [Kintzel \(2005\)](#). The optimisation routine could be applied iteratively in the GPA algorithm, which is essentially a sequence of pairwise Procrustes alignments, to obtain an *indefinite GPA*.

On the other hand, for directed and bipartite graphs, the criteria (4.2) and (4.3) must be optimised jointly for the two embeddings obtained using DASE in Definition 3. An approximated fast procedure for jointly optimising (4.2) iteratively for two embeddings $(\hat{\mathbf{X}}_1, \hat{\mathbf{Y}}_1)$ and $(\hat{\mathbf{X}}_2, \hat{\mathbf{Y}}_2)$ is described below:

1. *initialise* $\Omega^* = \mathbf{I}(d, 0)$, the identity matrix,
2. *repeat* until convergence in Ω^* :
 - (a) $\Omega^* \leftarrow \Omega^* \arg \min_{\Omega \in \mathbb{O}(d)} \|\hat{\mathbf{X}}_1 - \hat{\mathbf{X}}_2 \Omega^* \Omega\|_F$,
 - (b) $\Omega^* \leftarrow \Omega^* \arg \min_{\Omega \in \mathbb{O}(d)} \|\hat{\mathbf{Y}}_1 - \hat{\mathbf{Y}}_2 \Omega^* \Omega\|_F$.

Alternatively, the joint criterion should be optimised numerically. Note that the procedure could be also iterated obtaining a *joint generalised Procrustes algorithm*.

5 Improving prediction via fusion with edge specific information

The collapsed matrix used in (3.1) assumes that the underlying dynamics of each link are the same across the entire graph. This assumption is particularly limiting in real world applications, where different behaviours might be associated with different nodes or links. Instead, edge specific matrix parameters $\Psi_1, \dots, \Psi_T \in \mathbb{R}^{n \times n}$ might be able to more reliably capture the behaviour of each edge, providing a more flexible framework. An extended collapsed matrix $\tilde{\mathbf{A}}$ is obtained in this work as follows:

$$\tilde{\mathbf{A}} = \sum_{t=1}^T (\Psi_{T-t+1} \odot \mathbf{A}_t), \quad (5.1)$$

where Ψ_1, \dots, Ψ_T is a sequence of weighting matrices, and \odot represents the Hadamard element-wise product. Setting the last $T-p$ matrices Ψ_t to the matrix of zeros, $\tilde{\mathbf{A}}$ becomes an autoregression of order p .

The idea could be easily extended to other prediction settings, replacing the average link probability or average embedding with an autoregressive combination. For example, from the sequence of standard embeddings $\hat{\mathbf{X}}_1, \hat{\mathbf{X}}_2, \dots, \hat{\mathbf{X}}_T$, it could be possible to obtain the scores as follows:

$$\mathbf{S} = \sum_{t=1}^T \left(\Psi_{T-t+1} \odot \hat{\mathbf{X}}_t \hat{\mathbf{X}}_t^\top \right). \quad (5.2)$$

Alternatively, it could be possible to use a similar technique to provide an estimate $\tilde{\mathbf{X}}_{T+1}$ of the subsequent embedding \mathbf{X}_{T+1} , using the sequence of *aligned* embeddings $\hat{\mathbf{X}}_1, \hat{\mathbf{X}}_2, \dots, \hat{\mathbf{X}}_T$, and obtain the scores as:

$$\mathbf{S} = \tilde{\mathbf{X}}_{T+1} \tilde{\mathbf{X}}_{T+1}^\top. \quad (5.3)$$

Note that for this procedure to be meaningful, it is required to construct the individual ASEs using the same choices of d_+ and d_- for all the embeddings, which could be limiting in practical applications.

For estimation of the weighting matrices Ψ_1, \dots, Ψ_T , or the predicted \tilde{X}_{T+1} , two cases must be considered: the weights can be calculated from *real-valued* time series, for example the time series of inner products of the estimated embeddings for the two nodes forming a given edge, particularly relevant for (5.2), or from the *binary* time series of connections on a given edge, which arises when (5.1) is used. For simplicity, time series will be modelled independently. Studying the correlation structure between those entities is beyond the scope of this paper.

Seasonal ARIMA models (SARIMA, see, for example, Brockwell and Davis, 1987) represent a flexible modelling assumption. A time series Z_1, \dots, Z_T is a seasonal ARIMA(p, b, q)(P, B, Q) $_s$ with period s if the differenced series $\tilde{Z}_t = (1 - L)^b(1 - L^s)^B Z_t$, where L is the lag operator $L^k Z_t = Z_{t-k}$, is a causal ARMA process defined by the equation

$$\phi(L)\Phi(L^s)\tilde{Z}_t = \theta(L)\Theta(L^s)\varepsilon_t, \quad \varepsilon_t \stackrel{\text{iid}}{\sim} \mathbb{N}(0, \sigma^2), \quad (5.4)$$

where $\phi(v) = 1 - \phi_1 v - \dots - \phi_p v^p$, $\Phi(v) = 1 - \Phi_1 v - \dots - \Phi_P v^P$, $\theta(v) = 1 + \theta_1 v + \dots + \theta_q v^q$, and $\Theta(v) = 1 + \Theta_1 v + \dots + \Theta_Q v^Q$. Note that the process is causal if and only if $\phi(v) \neq 0$ and $\Phi(v) \neq 0$ for $|v| \leq 1$. The value of s usually depends on the application domain. In computer networks with daily network snapshots, $s = 7$, which represents a periodicity of one week. The remaining parameters, p, b, q, P, B and Q , could be estimated using AIC or BIC. For small values of T , the corrected AIC criterion (AICc) could be preferred. If s is unknown, information criteria could be also used for estimation. The corresponding coefficients of the polynomials $\phi(v)$, $\Phi(v)$, $\theta(v)$ and $\Theta(v)$, and the variance of the process σ^2 , can be estimated via maximum likelihood, using standard techniques in time series analysis (Brockwell and Davis, 1987). For an extensive discussion on automatic selection of the parameters in seasonal ARIMA models, see Hyndman and Khandakar (2008).

For prediction of future values Z_{t+1} , the general forecasting equation is obtained from (5.4) by using the relationship $\tilde{Z}_{t+1} = (1 - L)^b(1 - L^s)^B Z_{t+1}$, solving for Z_{t+1} , and setting ε_{t+1} to its expected value $\mathbb{E}(\varepsilon_{t+1}) = 0$, obtaining an estimate \hat{Z}_{t+1} from the known terms of the equation. k -steps ahead forecasts for Z_{t+k} can be obtained analogously.

Note that (5.1) and (5.2) are explicitly modelled using autoregressive coefficients, which is more restrictive than the generic form presented in (5.4). In this setting, the parameters could be estimated assuming a seasonal AR(p)(P) $_s$ model and using maximum likelihood with AIC or BIC penalisation, corresponding to the equation

$$\phi(L)\Phi(L^s)Z_t = \varepsilon_t, \quad \varepsilon_t \stackrel{\text{iid}}{\sim} \mathbb{N}(0, \sigma^2).$$

The AR form is preferred in this context for its interpretability over a model including a moving average term.

The SARIMA modelling approach might not be entirely appropriate for binary-valued time series, arising in (5.1). The literature in time series analysis has extensively discussed models for binary time series, surveyed, for example in MacDonald and Zucchini (1997). The most common approach is to assume that $A_{ijt} \stackrel{d}{\sim} \text{Bernoulli}(\pi_t)$, $\pi_t \in [0, 1]$, where the parameter π_t is then mapped to an underlying process z_t in \mathbb{R} using, for example, the probit or logistic transformations. The process z_t is then assumed to change dynamically according to an underlying process, which could be, for example, a SARIMA model. A popular choice is the dynamic binary response model of Kauppi and Saikkonen (2008). A more general framework for analysing non-Gaussian time series is provided by GARMA models (Benjamin et al., 2003).

On the other hand, the autoregressive form given to (5.1) does not allow to easily estimate the coefficients Ψ from the coefficients of a generalised process for binary time series, since the response is obtained from the parameters only through a transformation using a non-linear link function. Therefore, considering the form of (5.1), it seems more appropriate to treat the time series $\mathbf{A}_1, \mathbf{A}_2, \dots, \mathbf{A}_T$ as a standard SARIMA model, and estimate the coefficients Ψ using standard techniques for continuous-valued time series, even if the time series is binary. This choice has also relevant practical advantages, since most programming languages have packages for automatic estimation of the parameters in SARIMA models, whereas the choice of initial values and estimation of the parameters in most generalised process for binary time series is notoriously difficult, which is not desirable when the estimation task should be performed automatically and in parallel over a large set of time series.

6 Results

The proposed methods were tested on synthetic data and on two real world dynamic networks, the *Santander Cycles network* and the *Los Alamos National Laboratory user – destination IP graph*. The two networks come from two different domains of application: transportation systems and cybersecurity.

6.1 Simulated data

In this section, the performance of the multiple link prediction techniques discussed in this article is compared on simulated data from stochastic blockmodels. The stochastic blockmodel (Holland et al., 1983) can be interpreted as a special case of a GRDPG (Rubin-Delanchy et al., 2017): each node is assigned a latent community z_i , with corresponding latent position $\mu_{z_i} \in \mathbb{R}^d$, and the probability of a link (i, j)

only depends on the community allocation of the two nodes:

$$\mathbb{P}(A_{ij} = 1) = \boldsymbol{\mu}_{z_i}^\top \mathbf{I}(d_+, d_-) \boldsymbol{\mu}_{z_j}.$$

To simulate a stochastic blockmodel, a within-community probability matrix $\mathbf{B} = \{B_{ij}\} \in [0, 1]^{K \times K}$, where B_{ij} is the probability of a link between two nodes in communities i and j , and K is the number of communities, was generated from a beta distribution $\text{Beta}(1.2, 1.2)$. This choice of the parameters allows to have fairly heterogenous link probabilities in \mathbf{B} . The matrix has full rank with probability 1, hence $K = d$. In the simulation, $T = 100$ graph snapshots with $n = 100$ and $K = 5$ were generated. The community allocations were chosen to be time dependent, assuming a seasonality of one week. For each node, community allocations $z_{i,s}$, $s = 1, \dots, S$, with $S = 7$, were sampled at random from $\{1, \dots, K\}$. Then, the adjacency matrices were obtained as:

$$\mathbb{P}(A_{ijt} = 1) = B_{z_{i,t \bmod 7+1}, z_{j,t \bmod 7+1}}, \quad t = 1, \dots, T.$$

Therefore, the link probabilities change over time, with a periodicity of 7 days. The models presented in Section 3 were fitted using the first $T' = 80$ snapshots of the graph as training set, with the objective of predicting the remaining $T - T'$ adjacency matrices. The methods that are initially compared are:

- adjacency spectral embedding (3.2) of the *averaged adjacency matrix* (3.1) over the first T' snapshots,
- *averaged standard link score* (3.3), obtained from the average of the link probabilities calculated independently from the ASE for each \mathbf{A}_t ,
- *averaged standard embedding score* (3.4), obtained from the ASEs for $\mathbf{A}_1, \dots, \mathbf{A}_{T'}$,
- *averaged omnibus link score*, obtained from the average of the link probabilities calculated from the omnibus embedding,
- *averaged omnibus embedding score*, obtained from the averaged omnibus embedding of each node,
- *averaged COSIE score* (3.6) and (3.7), obtained from the average of the link probabilities calculated from the COSIE embedding.

The results are plotted in Figure 1. The link prediction problem can be framed as a binary classification task. Hence, the performance of the methods presented in this article is evaluated using *AUC scores* (Area Under the receiver operating characteristic Curve). Figure 1 shows that the best performance is achieved by the *averaged standard link scores*.

It is expected that the above methods are outperformed by the extensions presented in Section 5, since the network in this case has a clear dynamics which is not explicitly taken into account using the techniques in Section 3. In particular, four methods are discussed:

- adjacency spectral embedding of the *collapsed adjacency matrix* in (5.1), where the weights are obtained from independent seasonal $\text{AR}(p)(P)_7$ processes fitted on

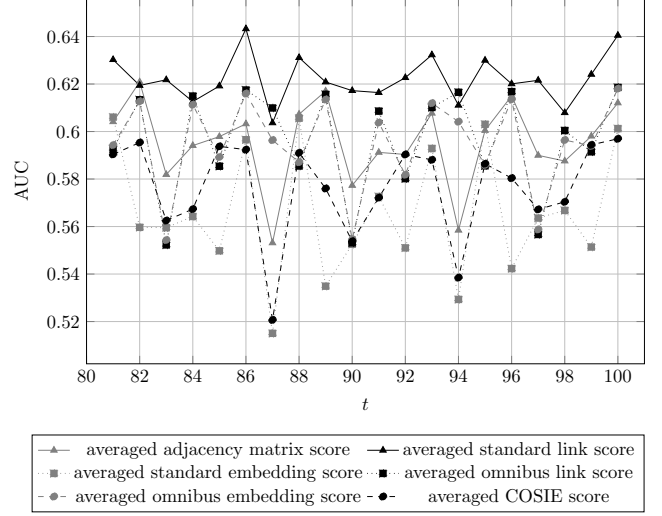


Figure 1: Results of the link prediction procedure on the simulated seasonal SBM.

each binary sequence $A_{ij1}, A_{ij2}, \dots, A_{ijT'}$ for all (i, j) such that at least one $A_{ijt} = 1$,

- prediction of the link prediction scores from the time series of scores $\hat{\mathbf{x}}_1^\top \hat{\mathbf{x}}_{j1}, \hat{\mathbf{x}}_2^\top \hat{\mathbf{x}}_{j2}, \dots, \hat{\mathbf{x}}_{T'}^\top \hat{\mathbf{x}}_{jT'}$ obtained from the individual ASEs on each $\mathbf{A}_1, \mathbf{A}_2, \dots, \mathbf{A}_{T'}$,
- prediction of the subsequent embeddings $\tilde{\mathbf{X}}_{T'+1}, \tilde{\mathbf{X}}_{T'+2}, \dots$ from the time series of *aligned*¹ individual ASEs $\tilde{\mathbf{X}}_1, \dots, \tilde{\mathbf{X}}_{T'}$, where independent models are fitted to the $n \times d$ time series corresponding to each entry, giving link prediction scores $\tilde{\mathbf{X}}_{T'+j} \tilde{\mathbf{X}}_{T'+j}^\top$, see (5.3),
- prediction of the subsequent COSIE correction matrices $\hat{\mathbf{R}}_{T'+1}, \hat{\mathbf{R}}_{T'+2}, \dots$ from the time series $\hat{\mathbf{R}}_1, \dots, \hat{\mathbf{R}}_{T'}$, where independent models are fitted to the $d \times d$ time series corresponding to each entry, giving link prediction scores $\tilde{\mathbf{X}} \hat{\mathbf{R}}_{T'+j} \tilde{\mathbf{X}}^\top$.

The time series models were fitted using the function `auto_arima` in the statistical *python* library `pmdarima`, using the corrected AIC criterion (AICc) to estimate the number of parameters. The results are presented in Figure 2.

The method of the *averaged standard link scores*, which had the best performance in Figure 1, is significantly improved using time series methods, and it is overall the only method that reaches values of the AUC well above 0.8. Remarkably, the performance of the *collapsed adjacency matrix* method in (5.1) outperforms the results based on most of the other methods, despite the issues related to the modelling of binary time series pointed out in Section 5. On the other hand, the improvements obtained using the *COSIE scores* and

¹The indefinite Procrustes alignment has been implemented in *python* using `rpy2` and the R codebase developed by Joshua Agterberg, available online at https://github.com/jagterberg/indefinite_procrustes and https://jagterberg.github.io/assets/procrustes_simulation.html. Last accessed: November 13, 2019.

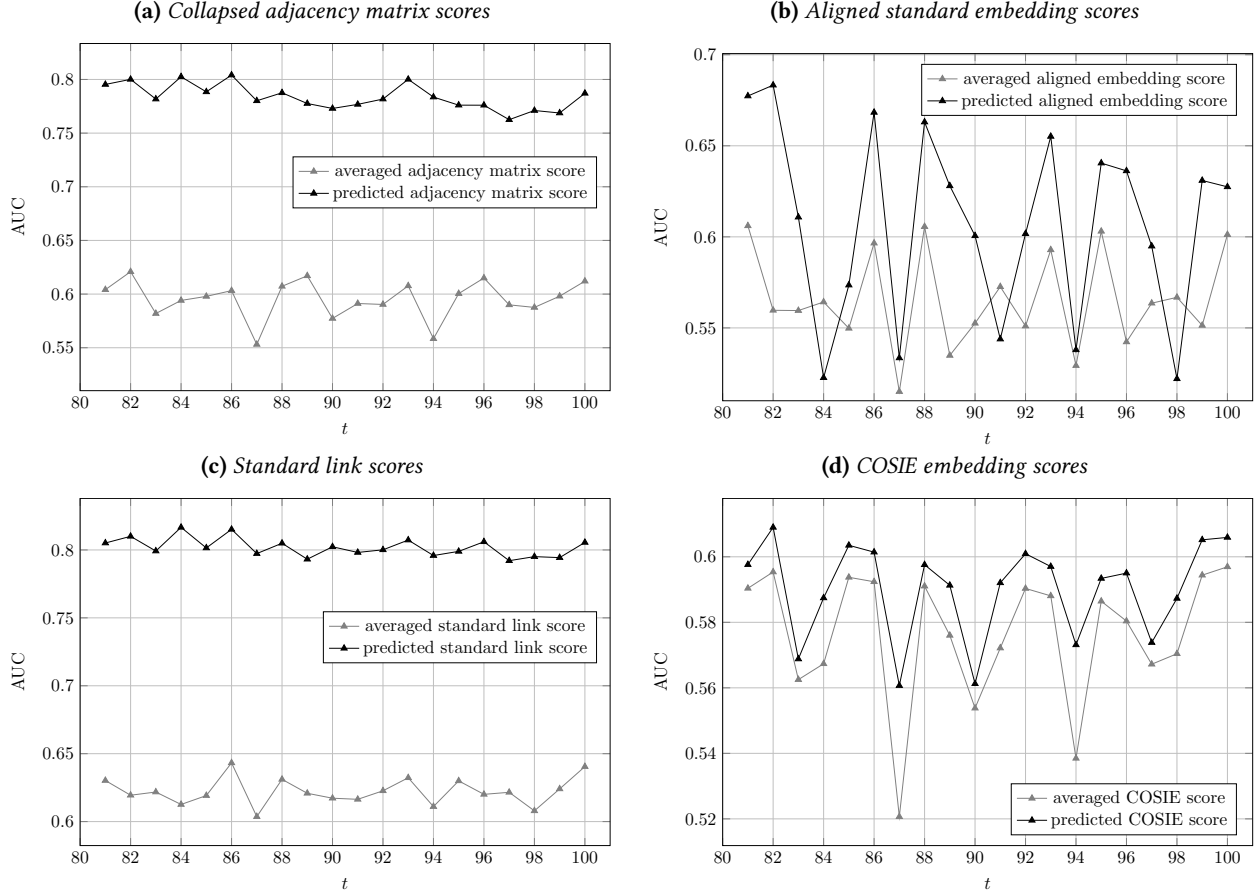


Figure 2: Comparison between four of the link prediction models in Figure 1, and their extensions using the methods in Section 5, on the synthetic SBM data.

especially the *aligned embedding scores* seem to be less significant compared to the two other methods. This aspect will also be confirmed on real data examples in the next section. In general, it is clear from the plots in Figure 2 that adding a temporal dynamics to the network via time series models is beneficial for link prediction purposes. In particular, including edge specific information from the time series of estimated link probabilities, or from the binary time series of links, has significantly improved the link prediction procedure. It seems more difficult to obtain significant improvements by directly predicting the embeddings.

6.2 Santander bikes

Santander Cycles is a self-service cycle hire scheme in central London. Data about usage of the bikes are periodically released by Transport for London². In this example, data from 7 March, 2018 to 19 March, 2019 were used, for a total of $T = 378$ days. Each bike sharing station is consid-

²The data are publicly available at <https://cycling.data.tfl.gov.uk/>, powered by TfL Open Data.

ered as a node, and an undirected edge (i, j, t) is drawn if at least one journey between the stations i and j is completed on day t . The total number of docking stations in London is $n = 840$. The graphs are fairly dense, with an average edge density of approximately 10% across the T networks. The first $T' = 250$ graphs are used as training set. Initially, the methods compared are four of the techniques used for Figure 1. For the Santander Cycles network, the results are reported in Figure 3.

Overall, this example seems to confirm that the method of the *averaged standard link score* (3.3) has the best performance for link prediction purposes, when time dynamics is not included. Notice that the performance of the classification procedure drops around day 294. This corresponds to Christmas day, which, not unexpectedly, has a different behaviour compared to non-festive days. It is also interesting to note that COSIE tends to perform better on weekdays than weekends, whereas the other methods predict more accurately the links on weekends compared to weekdays.

The results of the link prediction procedure in Figure 3 suggest that the data might not have a long term trend,

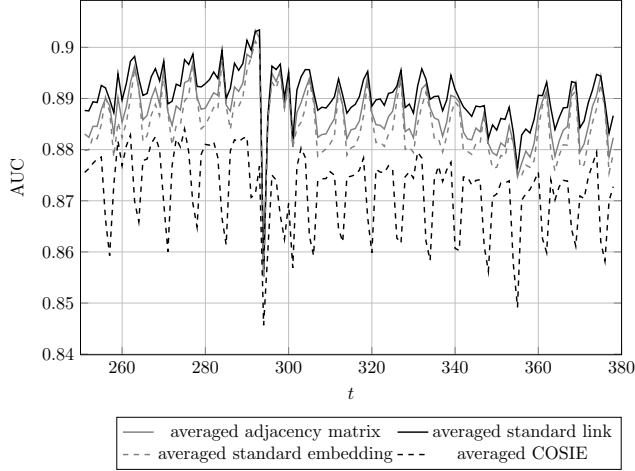


Figure 3: Results of the link prediction procedure on the Santander Cycles network.

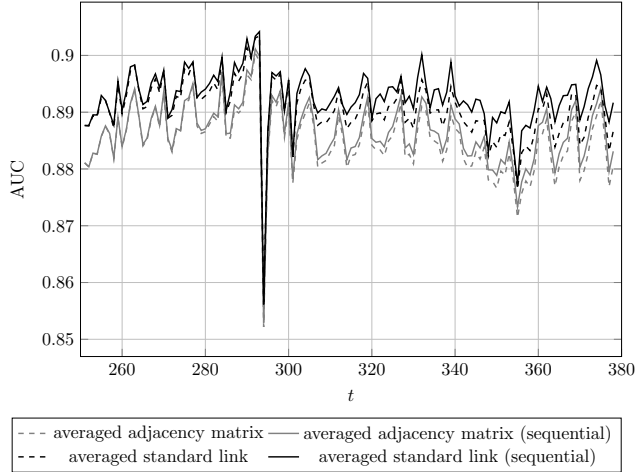


Figure 4: Results for the averaged adjacency matrix scores and averaged standard link scores procedures on the Santander Cycles network, with and without sequential updates.

but only a seasonal component, since the performance does not significantly decrease over time, and the parameters obtained using a training set of size $T' = 250$ seem to reliably predict the structure of the adjacency matrix even at $T = 378$. The performance could be improved by sequentially update the scores. An example with the *averaged adjacency matrix scores* and *averaged standard link scores* is given in Figure 4. Using the sequential scores is beneficial especially towards the end of the test set, whereas the difference between the two methodologies is negligible in the initial snapshots of the test set.

The performance of the classifiers could be again improved using some of the time series model in Section 5. The results obtained from the prediction of subsequent COSIE correction matrices, presented in Figure 5a, show that the

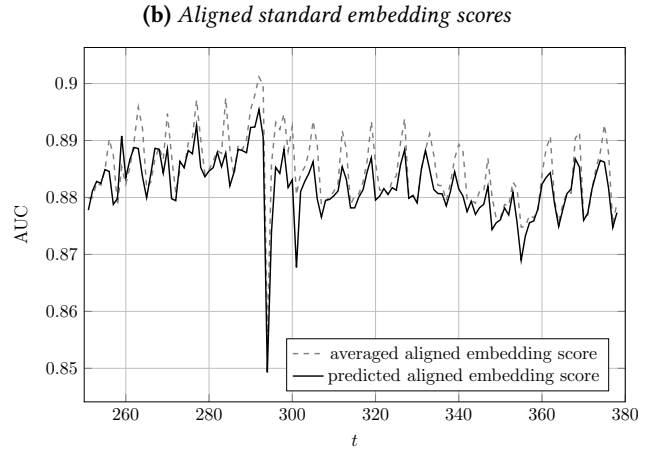
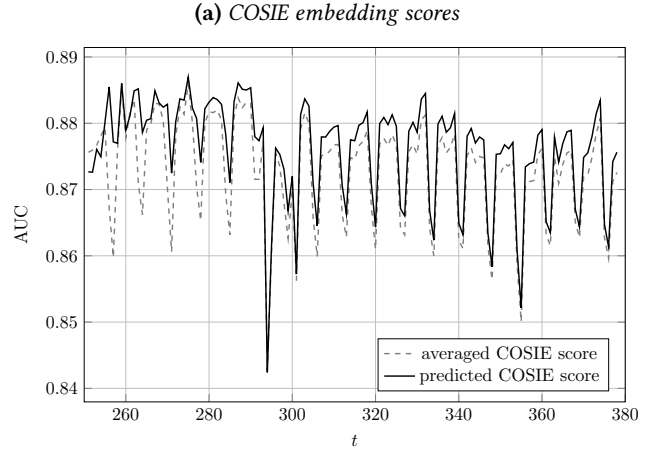


Figure 5: Comparison between two of the link prediction models in Figure 3, and their extensions using the methods in Section 5, on the Santander Cycles network.

predictive performance is slightly improved by the extended time series models. Again, it is empirically confirmed that adding temporal dynamics is beneficial for the performance of random dot product graph based classifiers.

On the other hand, predicting the subsequent adjacency spectral embeddings from the time series of aligned embeddings $\hat{\mathbf{X}}_1, \hat{\mathbf{X}}_2, \dots, \hat{\mathbf{X}}_{T'}$ does not improve the performance of the classifier, giving the result presented in Figure 5b. This confirms the results in Figure 2b, where the improvements on the simulated network were less significant compared to other methods. In this case, the time series models are not able to capture the dynamics of the aligned embedding, and the predictive performance does not improve in AUC.

The limited improvements in the results seem to suggest that the network does not have a strong dynamic component. The tradeoff between performance and the computational effort required to fit multiple independent time series simultaneously, would suggest to use the *sequential averaged*

standard link scores in practical applications.

6.3 Los Alamos National Laboratory unified host and network dataset

The unified host and network dataset released by the Los Alamos National Laboratory (Turcotte et al., 2018) consists in a collection of network flow and host event logs generated from machines running Microsoft Windows. From the host event logs, 90 daily user-authentication bipartite graphs have been constructed: $A_{ijt} = 1$ if the user i initiates a connection authenticating to computer j , on day t . This graph is also known as the *user – destination IP* graph. In this case, a total of $n_1 = 12,222$ users and $n_2 = 5,047$ hosts are observed. A total of 85,020 pairs (i, j) such that $A_{ijt} = 1$ for at least one $t \in \{1, \dots, T\}$ is observed, which corresponds to approximately 0.137% of all the possible links. The first $T' = 56$ matrices are used as training set. Note that it is computationally difficult to calculate $n_1 \times n_2$ scores for each adjacency matrix, and storing such large dense matrices in memory is also not efficient. Therefore, an estimate of the AUC could be obtained by subsampling the negative class at random from the zeroes in the test set adjacency matrices. Two subsampling techniques are used to construct the negative class for prediction of an adjacency matrix \mathbf{A}_t :

- (1) the negative class is simply constructed by randomly sampling pairs (i, j) such that $A_{ijt} = 0$,
- (2) the negative class contains a randomly selected set of pairs (i, j) such that $A_{ijt} = 0$, and all pairs (i, j) such that $A_{ijt} = 0$ and $A_{ijt'} = 1$ for at least 1 value of $t' \in \{1, \dots, T\}$.

For simplicity, the two techniques are denoted with the numbers (1) and (2) in Figure 6. The former method clearly provides an estimate of the ROC curve for the entire matrix, since the scores are sampled at random from the distribution of all the scores. On the other hand, the latter method includes in the negative class elements that tend to have associated high scores – represented by the pairs (i, j, t) such that $A_{ijt} = 0$, but $A_{ijt'} = 1$ for at least 1 value of $t' \in \{1, \dots, T\}$ –, giving an unbalanced sampling procedure and therefore a biased estimate of the ROC curve for the entire matrix. The methodology is still useful to compare the performance of different classifiers for a common negative class, providing a more challenging classification task when compared the subsampling method (1). Note that it is expected to obtain higher AUC scores using the first procedure, whereas the second procedure would return smaller values since the negative class includes links that had been otherwise observed in other snapshots of the graph.

Interestingly, in Figure 6a, the *average COSIE* scores seem to have the best predictive performance across the different methods. In particular, COSIE scores tend to largely outperform the other methods during weekdays, whereas the performance during weekends seems almost equivalent, and

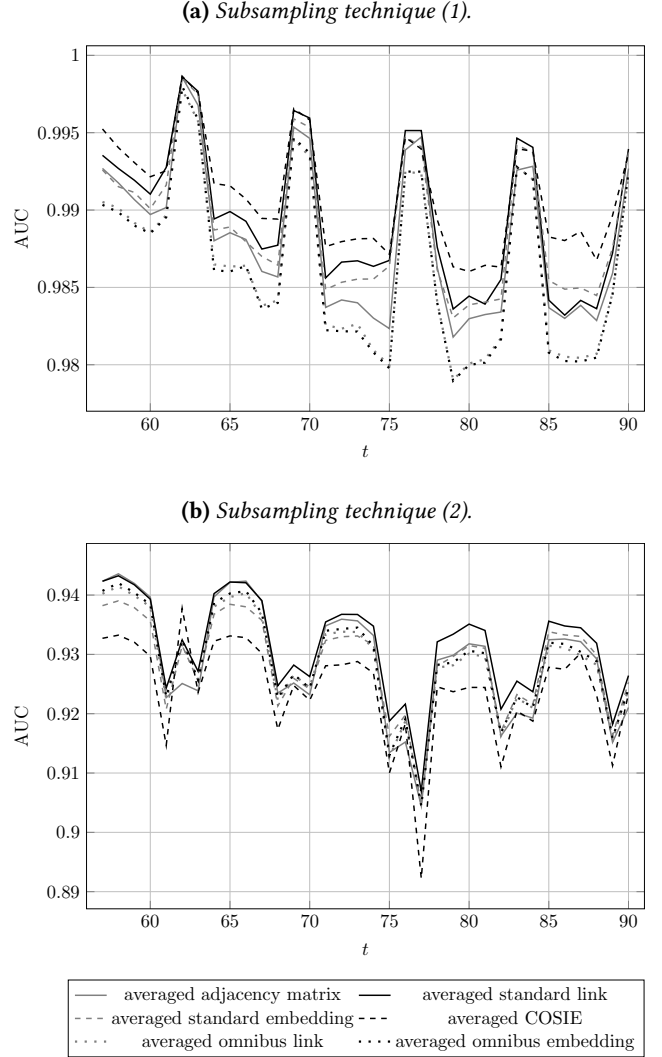


Figure 6: Results of the link prediction procedure on the LANL user – destination IP network. In both cases, AUCs were calculated from $\approx 150,000$ links per graph.

sometimes inferior, to the *average standard link* scores. On the other hand, in Figure 6b, COSIE scores have the worst performance among the methods, except a spike on day 62. In Figure 6b, *average standard link* scores give once again the best predictive performance. The results of Figure 6b are of particular interest since these allow for a comparison of the classifiers on a more challenging negative class compared to Figure 6a. Therefore, it is reasonable to conclude that *average standard link* scores emerge again as the most suitable method for link prediction based on random dot product graphs.

The link prediction procedure is clearly more effective when the scores are calculated sequentially, as Figure 7 shows. Note that the decreasing trend in the non-sequential

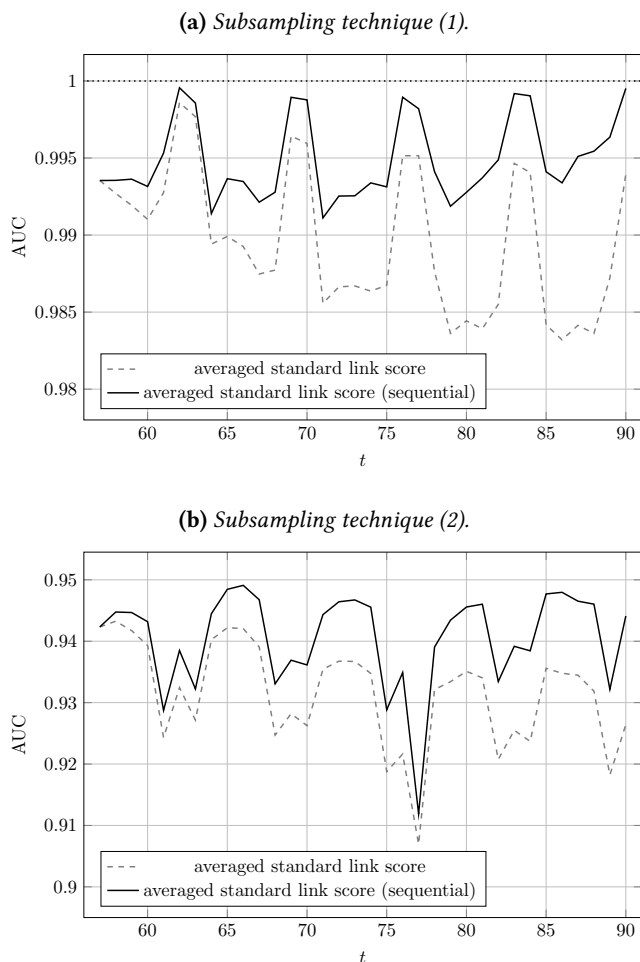


Figure 7: Results for the averaged standard link scores procedures on the LANL user – destination IP network, with and without sequential updates. AUCs were calculated from $\approx 150,000$ links per graph.

scores in Figure 6 and 7 might suggest that the graph has a relevant temporal dynamics.

The performance of the different methods can be again improved using the time series models in Section 5. In particular, Figure 8 shows the results obtained using the two different subsampling schemes and the *collapsed adjacency matrix scores*, *standard link scores* and *COSIE scores*. From Figures 8a, 8c and 8e, it is evident that the extensions do not improve the performance of the classifier when the subsampling scheme (1) is used. On the other hand, Figures 8b, 8d and 8f show that relevant improvements (especially on day 62) are obtained when the subsampling method (2) is used, which represents a more difficult classification task. Again, the results confirm that the performance of random dot product graph models can be enhanced by edge-based time series models.

7 Conclusion

In this paper, link prediction techniques based on random dot product graphs have been presented, discussed and compared. In particular, link prediction methods based on sequences of aligned embeddings, COSIE networks, and omnibus embeddings have been proposed. Applications on simulated and real world datasets have shown that one of the most common approaches used in the literature, the decomposition of a *collapsed adjacency matrix* $\tilde{\mathbf{A}}$, is usually outperformed by other methods based on random dot product graphs. The *average standard link scores* – obtained as the average of the inner products from sequences of individual embeddings of snapshots of the graph – have given the best performance in terms of AUC scores across multiple datasets. This result is particularly appealing for practical applications: calculating the individual ASEs is computationally inexpensive using algorithms for large sparse matrices, and the method seems particularly suitable for implementation in a *streaming* fashion, since the average link score could be easily updated on the run when new snapshots of the graph are observed. The methods discussed in the article have then been further extended to include temporal dynamics at the edge level, using time series models. The extensions have shown improvements over standard random dot product graph based link prediction techniques, especially when the graph exhibits a strong dynamic component. Overall, this paper provides guidelines for practitioners for using random dot product graphs as tools for link prediction in networks, providing insights into the predictive capability of such statistical network models.

Acknowledgements

FSP acknowledges funding from the EPSRC.

References

- Arroyo-Reli3n, J. D., Athreya, A., Cape, J., Chen, G., Priebe, C. E. and Vogelstein, J. T. (2019) Inference for multiple heterogeneous networks with a common invariant subspace. *arXiv e-prints*, arXiv:1906.10026.
- Arroyo-Reli3n, J. D., Kessler, D., Levina, E. and Taylor, S. F. (2017) Network classification with applications to brain connectomics. *arXiv e-prints*.
- Athreya, A., Fishkind, D. E., Tang, M., Priebe, C. E., Park, Y., Vogelstein, J. T., Levin, K., Lyzinski, V., Qin, Y. and Sussman, D. L. (2018) Statistical inference on random dot product graphs: a survey. *Journal of Machine Learning Research*, **18**, 1–92.

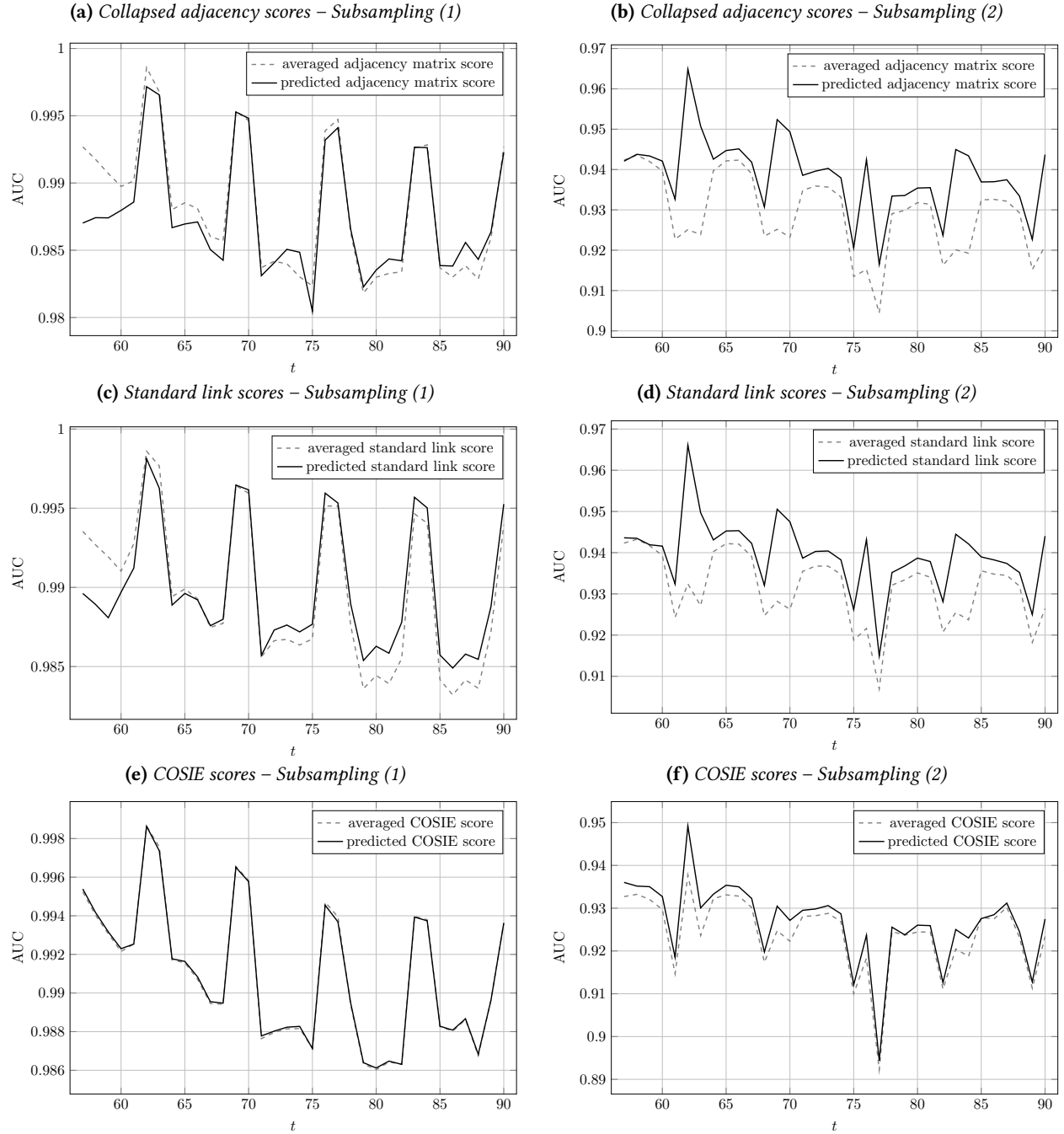


Figure 8: Comparison between three of the link prediction models in Figure 6, and their extensions using the methods in Section 5, on the LANL user – destination IP network. AUCs were calculated from $\approx 150,000$ links per graph.

- Benjamin, M. A., Rigby, R. A. and Stasinopoulos, D. M. (2003) Generalized autoregressive moving average models. *Journal of the American Statistical Association*, **98**, 214–223.
- Brockwell, P. J. and Davis, R. A. (1987) *Time Series: Theory and Methods*. Springer Series in Statistics. Springer-Verlag.
- Charlin, L., Ranganath, R., McInerney, J. and Blei, D. M. (2015) Dynamic Poisson factorization. In *Proceedings of the 9th ACM Conference on Recommender Systems*, 155–162. ACM.
- Clauset, A., Moore, C. and Newman, M. E. J. (2008) Hierarchical structure and the prediction of missing links in networks. *Nature*, **453**.
- Dhillon, I. S. (2001) Co-clustering documents and words using bipartite spectral graph partitioning. In *Proceedings of the Seventh ACM SIGKDD Conference on Knowledge Discovery and Data Mining*, KDD '01, 269–274. New York, NY, USA: ACM.
- Dong, X., Frossard, P., Vandergheynst, P. and Nefedov, N. (2014) Clustering on multi-layer graphs via subspace analysis on grassmann manifolds. *IEEE Transactions on Signal Processing*, **62**, 905–918.
- Dryden, I. L. and Mardia, K. V. (2016) *Statistical Shape Analysis, with Applications in R. Second Edition*. Chichester: John Wiley and Sons.
- Dunlavy, D. M., Kolda, T. G. and Acar, E. (2011) Temporal link prediction using matrix and tensor factorizations. *ACM Transactions on Knowledge Discovery from Data*, **5**.
- Durante, D. and Dunson, D. B. (2014) Nonparametric Bayes dynamic modelling of relational data. *Biometrika*, **101**, 883–898.
- (2018) Bayesian inference and testing of group differences in brain networks. *Bayesian Analysis*, **13**, 29–58.
- Durante, D., Dunson, D. B. and Vogelstein, J. T. (2017) Nonparametric bayes modeling of populations of networks. *Journal of the American Statistical Association*, **112**, 1516–1530.
- Ginestet, C. E., Li, J., Balachandran, P., Rosenberg, S. and Kocaczyk, E. D. (2017) Hypothesis testing for network data in functional neuroimaging. *Annals of Applied Statistics*, **11**, 725–750.
- Gower, J. C. (1975) Generalized Procrustes analysis. *Psychometrika*, **40**, 33–51.
- Heard, N. A., Adams, N., Rubin-Delanchy, P. and Turcotte, M. J. M. (2018) *Data Science for Cyber-Security*. World Scientific (Europe).
- Hoff, P. D., Raftery, A. E. and Handcock, M. S. (2002) Latent space approaches to social network analysis. *Journal of the American Statistical Association*, **97**, 1090–1098.
- Holland, P. W., Laskey, K. B. and Leinhardt, S. (1983) Stochastic blockmodels: First steps. *Social Networks*, **5**, 109 – 137.
- Hosseini, S. A., Khodadadi, A., Alizadeh, K., Arabzadeh, A., Farajtabar, M., Zha, H. and Rabiee, H. R. (2018) Recurrent Poisson factorization for temporal recommendation. *IEEE Transactions on Knowledge and Data Engineering*.
- Hyndman, R. and Khandakar, Y. (2008) Automatic time series forecasting: The forecast package for R. *Journal of Statistical Software, Articles*, **27**, 1–22.
- Ishiguro, K., Iwata, T., Ueda, N. and Tenenbaum, J. B. (2010) Dynamic infinite relational model for time-varying relational data analysis. In *Advances in Neural Information Processing Systems 23* (eds. J. D. Lafferty, C. K. I. Williams, J. Shawe-Taylor, R. S. Zemel and A. Culotta), 919–927. Curran Associates, Inc.
- Jeske, D. R., Stevens, N. T., Tartakovsky, A. G. and Wilsson, J. D. (2018) Statistical methods for network surveillance. *Applied Stochastic Models in Business and Industry*, **34**, 425–445.
- Kauppi, H. and Saikkonen, P. (2008) Predicting U.S. recessions with dynamic binary response models. *The Review of Economics and Statistics*, **90**, 777–791.
- Kim, Y. and Levina, E. (2019) Graph-aware Modeling of Brain Connectivity Networks. *arXiv e-prints*.
- Kintzel, U. (2005) Procrustes problems in finite dimensional indefinite scalar product spaces. *Linear Algebra and its Applications*, **402**, 1–28.
- Krivitsky, P. N. and Handcock, M. S. (2014) A separable model for dynamic networks. *Journal of the Royal Statistical Society: Series B (Statistical Methodology)*, **76**, 29–46.
- Levin, K., Athreya, A., Tang, M., Lyzinski, V., Park, Y. and Priebe, C. E. (2017) A central limit theorem for an omnibus embedding of multiple random graphs and implications for multiscale network inference. *arXiv e-prints*, arXiv:1705.09355.
- Liben-Nowell, D. and Kleinberg, J. (2007) The link-prediction problem for social networks. *Journal of the American Society for Information Science and Technology*, **58**, 1019–1031.
- Lü, L. and Zhou, T. (2011) Link prediction in complex networks: A survey. *Physica A: Statistical Mechanics and its Applications*, **390**, 1150 – 1170.

- MacDonald, I. L. and Zucchini, W. (1997) *Hidden Markov and Other Models for Discrete-valued Time Series*. Chapman & Hall/CRC Monographs on Statistics & Applied Probability. Taylor & Francis.
- Menon, A. K. and Elkan, C. (2011) Link prediction via matrix factorization. In *Machine Learning and Knowledge Discovery in Databases: European Conference, ECML PKDD 2011, Part II* (eds. D. Gunopulos, T. Hofmann, D. Malerba and M. Vazirgiannis), 437–452. Berlin, Heidelberg: Springer Berlin Heidelberg.
- Metelli, S. and Heard, N. A. (2019) On Bayesian new edge prediction and anomaly detection in computer networks. *Annals of Applied Statistics*, **13**, 2586–2610.
- Neil, J., Hash, C., Brugh, A., Fisk, M. and Storlie, C. B. (2013) Scan statistics for the online detection of locally anomalous subgraphs. *Technometrics*, **55**, 403–414.
- Nielsen, A. M. and Witten, D. (2018) The multiple random dot product graph model. *arXiv e-prints*.
- Rubin-Delanchy, P., Priebe, C. E., Tang, M. and Cape, J. (2017) A statistical interpretation of spectral embedding: the generalised random dot product graph. *ArXiv e-prints*.
- Sarkar, P. and Moore, A. W. (2006) Dynamic social network analysis using latent space models. In *Advances in Neural Information Processing Systems 18* (eds. Y. Weiss, B. Schölkopf and J. C. Platt), 1145–1152. MIT Press.
- Schein, A., Paisley, J., Blei, D. M. and Wallach, H. (2015) Bayesian Poisson tensor factorization for inferring multilateral relations from sparse dyadic event counts. In *Proceedings of the 21th ACM SIGKDD International Conference on Knowledge Discovery and Data Mining*, 1045–1054. ACM.
- Schein, A., Zhou, M., Blei, D. M. and Wallach, H. (2016) Bayesian Poisson tucker decomposition for learning the structure of international relations. In *Proceedings of the 33rd International Conference on Machine Learning*, New York, NY, USA.
- Scheinerman, E. R. and Tucker, K. (2010) Modeling graphs using dot product representations. *Computational Statistics*, **25**, 1–16.
- Schönemann, P. H. (1966) A generalized solution of the orthogonal Procrustes problem. *Psychometrika*, **31**, 1–10.
- Sewell, D. K. and Chen, Y. (2015) Latent space models for dynamic networks. *Journal of the American Statistical Association*, **110**, 1646–1657.
- Sharan, U. and Neville, J. (2008) Temporal-relational classifiers for prediction in evolving domains. In *Proceedings of the 2008 Eighth IEEE International Conference on Data Mining, ICDM '08*, 540–549. Washington, DC, USA: IEEE Computer Society.
- Shiga, M. and Mamitsuka, H. (2012) A variational Bayesian framework for clustering with multiple graphs. *IEEE Transactions on Knowledge and Data Engineering*, **24**, 577–590.
- Tang, R., Ketcha, M., Badea, A., Calabrese, E. D., Margulies, D. S., Vogelstein, J. T., Priebe, C. E. and Sussman, D. L. (2019) Connectome Smoothing via Low-rank Approximations. *IEEE Transactions on Medical Imaging*, **38**, 1446–1456.
- Tang, W., Lu, Z. and Dhillon, I. S. (2009) Clustering with multiple graphs. In *Proceedings of the 2009 Ninth IEEE International Conference on Data Mining, ICDM '09*, 1016–1021. Washington, DC, USA: IEEE Computer Society.
- Turcotte, M. J. M., Kent, A. D. and Hash, C. (2018) *Unified Host and Network Data Set*, chap. 1, 1–22. World Scientific.
- Wang, S., Arroyo-Relión, J. D., Vogelstein, J. T. and Priebe, C. E. (2019) Joint Embedding of Graphs. *IEEE Transactions on Pattern Analysis and Machine Intelligence*, **to appear**.
- Xing, E. P., Fu, W. and Song, L. (2010) A state-space mixed membership blockmodel for dynamic network tomography. *Annals of Applied Statistics*, **4**, 535–566.
- Xu, K. S. and Hero III, A. O. (2014) Dynamic stochastic blockmodels for time-evolving social networks. *IEEE Journal of Selected Topics in Signal Processing*, **8**, 552–562.
- Young, S. J. and Scheinerman, E. R. (2007) Random dot product graph models for social networks. In *Algorithms and Models for the Web-Graph* (eds. A. Bonato and F. R. K. Chung), 138–149. Springer Berlin Heidelberg.